

Novel PI3K and mTOR Inhibitor NVP-BEZ235 Radiosensitizes Breast Cancer Cell Lines under Normoxic and Hypoxic Conditions

Sebastian Kuger¹, Emre Cörek¹, Bülent Polat^{1,3}, Ulrike Kämmerer², Michael Flentje¹
and Cholpon S. Djuzenova¹

¹Department of Radiation Oncology, University Hospital of Würzburg, Würzburg, Germany. ²Department of Obstetrics and Gynaecology, University Hospital of Würzburg, Würzburg, Germany. ³Comprehensive Cancer Center Mainfranken, University of Würzburg, Würzburg, Germany.

ABSTRACT: In the present study, we assessed, if the novel dual phosphatidylinositol 3-kinase (PI3K)/mammalian target of rapamycin (mTOR) inhibitor NVP-BEZ235 radiosensitizes triple negative (TN) MDA-MB-231 and estrogen receptor (ER) positive MCF-7 cells to ionizing radiation under various oxygen conditions, simulating different microenvironments as occurring in the majority of breast cancers (BCs). Irradiation (IR) of BC cells cultivated in hypoxic conditions revealed increased radioresistance compared to normoxic controls. Treatment with NVP-BEZ235 completely circumvented this hypoxia-induced effects and radiosensitized normoxic, reoxygenated, and hypoxic cells to similar extents. Furthermore, NVP-BEZ235 treatment suppressed HIF-1 α expression and PI3K/mTOR signaling, induced autophagy, and caused protracted DNA damage repair in both cell lines in all tested oxygen conditions. Moreover, after incubation with NVP-BEZ235, MCF-7 cells revealed depletion of phospho-AKT and considerable signs of apoptosis, which were significantly enhanced by radiation. Our findings clearly demonstrate that NVP-BEZ235 has a clinical relevant potential as a radiosensitizer in BC treatment.

KEYWORDS: radiosensibility, Akt, DNA repair protraction, apoptosis, hypoxia, autophagy

CITATION: Kuger et al. Novel PI3K and mTOR Inhibitor NVP-BEZ235 Radiosensitizes Breast Cancer Cell Lines under Normoxic and Hypoxic Conditions. *Breast Cancer: Basic and Clinical Research* 2014;8:39–49 doi: 10.4137/BCBCR.S13693.

RECEIVED: November 21, 2013. **RESUBMITTED:** January 23, 2014. **ACCEPTED FOR PUBLICATION:** January 24, 2014.

ACADEMIC EDITOR: Goberdhan P. Dimri, Editor in Chief

TYPE: Original Research

FUNDING: The hypoxic glove boxes were supported by a grant of the interdisciplinary Centre of Clinical research (iZKF) of the University of Würzburg. This publication was funded by the German Research Foundation (DFG) and the University of Würzburg in the funding programme Open Access Publishing.

COMPETING INTERESTS: Author(s) disclose no potential conflicts of interest.

COPYRIGHT: © the authors, publisher and licensee Libertas Academica Limited. This is an open-access article distributed under the terms of the Creative Commons CC-BY-NC 3.0 License.

CORRESPONDENCE: Kuger_S@ukw.de

Introduction

Although breast cancer (BC) mortality rates are decreasing, most likely because of efficient screening strategies, BC still is the leading cause of cancer-related deaths in women worldwide.¹ Current BC therapy depends on the type and stage of the BC and traditionally consists of a multivariate approach including surgery, hormone therapy, systemic chemotherapy, radiotherapy, and molecular targeted therapy.² However, one prerequisite for a hormone therapy is the expression of estrogen or progesterone receptors (ER and PgR, respectively) in the cancer cells. These ER and PgR positive cancers account for about 75–80% of the diagnosed BCs, whereas about 10–15% are diagnosed as triple negative (TN) BC.

These subtypes of BC lack not only the expression of ER and PgR, but also overexpression of human epidermal growth factor receptor 2 (HER2). Currently, chemo- and molecular-targeted therapies are the only systemic approaches for these malignancies.^{3,4}

One promising molecular target is the phosphatidylinositol 3-kinase (PI3K)/Akt/mammalian target of rapamycin (mTOR) pathway, because it is frequently mutated in human cancers and its activation alters a number of cellular processes that are stimulating proliferation, cell growth, and survival.⁵ Furthermore, activation of this pathway has been shown to decrease sensitivity to chemotherapeutics as well as to irradiation (IR),^{6,7} resulting in diminished treatment success.

However, radiosensitivity is determined not only by the cells' intrinsic radioresistance, which can be modulated with radiosensitizing agents, but also by the surrounding microenvironment, especially by the oxygen saturation. According to Vaupel et al., a median oxygen partial pressure of 65 mmHg (8.67 kPa) and 30 mmHg (4.00 kPa) was observed in normal breast and BC tissue,⁸ corresponding to an oxygen content of 8.5 and 4.0%, respectively. However, oxygen concentration within these hypoxic areas differs with the biggest subgroup showing a partial pressure of about 5–7.5 mmHg (0.66–1.00 kPa),⁸ which confers to an oxygen content of about 1%. Especially, these hypoxic regions in solid malignancies, as occurring in about 40% of all BC,⁹ reveal various changes in pro-survival gene expression, suppressed apoptosis, as well as increased invasiveness, metastasis, and genomic instability.^{10,11}

In solid tumors, three different cell subpopulations exist because of changes in the microregional blood flow: normoxic cells, cells that are subjected to intermittent hypoxia and hypoxic cells.^{12–14} Because these subpopulations differ in their biology and have different resistances to chemo- and radiotherapy, all three should be taken into account, when investigating the efficiency of novel drugs.^{15–17}

The hypoxia-induced changes, which are linked to increased radioresistance, are intertwined with the PI3K/Akt/mTOR pathway, outlining this signaling network as a promising target for a radiosensitizing approach in normoxic and hypoxic conditions.^{18–20} In fact, the novel orally available dual PI3K/mTOR inhibitor NVP-BEZ235, which is currently used in clinical trials as a chemotherapeutic drug,²¹ already showed promising cytostatic results in BC treatment,^{22,23} and revealed a radiosensitizing potential in hypopharyngeal and prostate cancer cells under normoxic and harsh hypoxic conditions.^{24,25} However, no study is published yet that validated these promising results in the physiological relevant conditions of mild intermittent hypoxia in BC cell lines.⁸

To prove whether the dual PI3K/mTOR inhibitor radiosensitizes BC cells, we treated TN MDA-MB-231 and ER-positive MCF-7 cells with NVP-BEZ235, concomitantly simulating the clinically relevant oxygenation states of

normoxic, reoxygenated after IR, and hypoxic tumor cells. After determining the cytotoxicity of NVP-BEZ235, we cultured cells in normoxic, reoxygenated, or hypoxic conditions and assessed the colony-forming ability, the cell cycle distributions, and the induction and decay of DNA double-strand breaks (DSBs) after IR. Furthermore, we investigated the incidence of apoptosis markers (hypodiploid cells and poly (ADP-ribose) polymerase (PARP) cleavage), and the expression of the hypoxia-inducible factor 1-alpha (HIF-1 α), several PI3K/Akt/mTOR pathways (PI3K p110, PI3k p85, p-Akt, Akt, p-mTOR, mTOR, p-S6, S6, and p-4E-BP1), and autophagy-related proteins (LC3-I and LC3-II).

Materials and Methods

Cell culture and drug treatment. The human BC cell lines MCF-7 and MB-231 were obtained from the “Cell Lines Services” company (Heidelberg, Germany) and routinely cultured under standard conditions (37 °C, 5% CO₂) in complete growth medium (CGM), which was Dulbecco's modified Eagle's medium supplemented with 10% fetal bovine serum and 5% glutamine. To compare normoxic, reoxygenated, and hypoxic cells, 5 × 10⁵ cells were allowed to attach in standard 75 cm² tissue culture flasks (Greiner Bio-One, Frickenhausen, Germany) for six hours before cells for reoxygenation and hypoxia experiments were transferred into a hypoxic glove box (Coy Laboratory Products, Grass Lake, USA) and cultured at 1% O₂, which is a partial pressure of approximately 8 mmHg, thus reflecting a mild hypoxia in tumor tissue, overnight. For reoxygenation, experiments cells were incubated under standard conditions after IR, whereas cells of hypoxia experiments were further cultured at 1% O₂ after IR until harvest or seeding in the case of colony-forming assays (compare Figure 1).

For all experiments, except cell viability assay, cells were treated one hour before IR with 100 nM of the dual PI3K/mTOR inhibitor NVP-BEZ235,²⁶ which was provided by Novartis Institutes for BioMedical Research (Basel, Switzerland). The drug was freshly diluted from frozen aliquots stored at –20 °C. Cells treated in parallel with respective amounts of dimethyl sulfoxide (DMSO) served as controls.

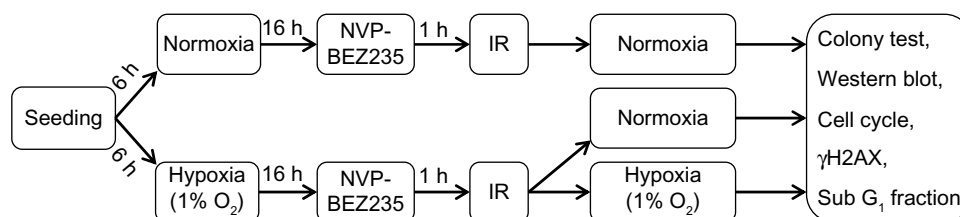


Figure 1. A flowchart of cell culture in this study. Normoxic cells were kept under 21% O₂ throughout the experiment. For the reoxygenation setup, cells were kept under hypoxic conditions (1% O₂) until IR and were cultivated at 21% O₂ afterward. For the hypoxia experiments, cells were cultivated in hypoxic conditions before and after IR. In all oxygenation setups, cells were treated with 100 nM NVP-BEZ235 one hour before IR. For colony-forming assays, cells were cultivated for 24 hours after IR in indicated oxygen concentrations before plating of the cells. For Western blot, cell cycle, γ H2AX, and sub G1 measurements cells were fixed at 30 minutes, 24 hours, and 48 hours after IR.

X-ray IR. IR was performed at room temperature using a 6-MV Siemens linear accelerator (Siemens, Concord, USA) at a dose rate of 2 Gy/minute. After IR, cells were kept in CGM according to the treatment schedule, for the indicated time until harvest.

Cell viability assay. To examine the cytotoxic effects of NVP-BEZ235, we used the CellTiter 96 AQueous One Solution (Promega, Madison, USA) according to the manufacturer's instructions. Serial dilutions of NVP-BEZ235 (6.25–800 nM) in CGM were added to normoxic (21% O₂) and hypoxic (1% O₂) cell cultures in quadruplicates, and the cytotoxicity of the drug was determined 24 hours later. Further analysis of the data was basically as described previously.²⁷

Colony-forming assay. Colony-forming assay was performed, and data were analyzed as described elsewhere.^{27,28} Briefly, subconfluent monolayers of cells were treated with 100 nM NVP-BEZ235 or respective amounts of DMSO one hour before IR with graded single doses (0–8 Gy) at room temperature. Twenty-four hours after IR, cells were seeded in Petri dishes and cultivated in CGM under standard conditions for two weeks. Colonies were stained with 0.6% crystal violet, and colonies containing more than 50 cells were scored as survivors. Experiments were done in quadruplicate, and each experiment was repeated at least three times.

Western blot. After preparation of nuclear extracts or whole cell lysates according to standard protocols, samples equivalent to 10–40 µg of protein were separated according to their protein size using 4–12% sodium-dodecyl-sulfate-polyacrylamide pre-cast gels (Invitrogen, Karlsruhe, Germany) and transferred to nitrocellulose membranes. Membranes were incubated with protein-specific primary and species-specific peroxidase-labeled secondary antibody for protein detection. The protein expression levels were quantified using ImageJ (NIH, Bethesda, USA), and protein expression was normalized to the levels of β-tubulin (nuclear extracts) or β-actin (whole cell lysates).

Antibodies. The antibodies used in the experiments of this article are specified in the electronic supplementary material (ESM).

Detection of histone γH2AX, cell cycle distribution, and measurement of hypodiploid cell fraction by flow cytometry. To quantify IR and/or drug-induced DNA DSBs, we assessed the phosphorylation of the histone H2AX.²⁹ To this end, drug-treated and DMSO-treated cells were fixed for further analysis at 30 minutes, 24 hours, and 48 hours after IR. Staining and analysis of the fixed samples were performed essentially as described elsewhere.³⁰ Cells were counterstained with 4',6-diamidino-2-phenylindole dihydrochloride (DAPI) (Sigma-Aldrich, Munich, Germany) in the presence of RNase A (Sigma-Aldrich, Munich, Germany), to assess cell cycle distribution and to quantify cells with a hypodiploid DNA content. At least 20,000 cells were assessed simultaneously for histone γH2AX and DNA content using a flow cytometer FACSCanto II (Becton Dickinson, San Jose, USA). Analysis

of the acquired data, calculation of the geometric mean fluorescence intensity (MFI) of FITC, and deconvolution of DNA histogram were performed using the Flowing Software program obtained from P. Terho (Turku Centre for Biotechnology, Turku, Finland) and the ModFit LT program (Verity Software House, Topsham, USA).

Statistics. Data are presented as means ± standard deviation of at least three independent experiments. Unpaired *t*-tests were performed, and *P*-value less than 0.05 was considered to be statistically significant. For multiple comparisons, Holm-Bonferroni method of alpha error correction was applied. Statistics and fitting of experimental data were performed with RStudio 0.96.331 (Free Software Foundation, Boston, USA) and Origin 8.5 (Microcal, Northampton, USA).

Results

NVP-BEZ235 decreased cell proliferation and sensitized cells to IR independent of oxygen supply. To assess the effects of NVP-BEZ235 on proliferation of MDA-MB-231 and MCF-7 cells, we treated both cell lines with serial dilutions of the dual inhibitor within a concentration range of 6.25–800 nM and quantified cell viability by an 3-(4,5-dimethylthiazol-2-yl)-5-(3-carboxymethoxyphenyl)-2-(4-sulfophenyl)-2H-tetrazolium (MTS)-based assay. Formazan production, detected by absorbance at 492 nm, in drug-treated samples was normalized against controls treated with DMSO and plotted versus drug concentration. As evident from Figure 2, incubation of normoxic cells for 24 hours with increasing NVP-BEZ235 concentrations decreased cell proliferation to about 75 and 65% of the initial level in MDA-MB-231 and MCF-7 cells, respectively. Interestingly, drug exposure in hypoxic culture conditions resulted in superior growth inhibition, compared to normoxic samples, to about 55% of the control levels in both cell lines. For subsequent experiments, we used a drug concentration of 100 nM, which inhibited cell proliferation to about 80% of the maximal effect (IC₈₀) in both cell lines and which is in line with previously published experiments.^{26,27,31}

To ensure that the radiosensitivity of the examined cell lines depends on oxygen saturation, we performed colony formation assays with cells cultured in different oxygen conditions. As shown in Figure 3, hypoxic cells were more resistant to radiation, showing increased surviving fractions depending on the oxygen partial pressure. For the following hypoxia and reoxygenation experiments, we used an oxygen concentration of 1%, which showed statistical significant differences in terms of radiosensitivity compared to normoxic controls and which is in line with the predominant physiological condition of a mild hypoxia in BC.⁸

To address the question, whether treatment with 100 nM NVP-BEZ235 sensitizes the BC cell lines to IR and if this radiosensitization is affected by the oxygenation status, we performed colony-forming assays (Fig. 4A). Hypoxic culture conditions were validated by elevated HIF-1α expression in

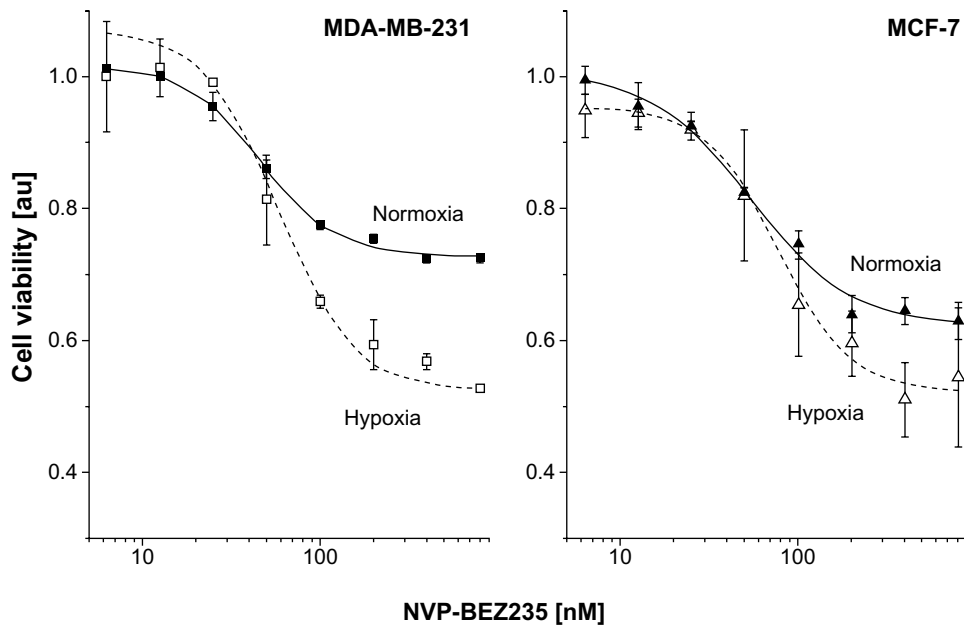


Figure 2. Effect of 24 hours of exposure to serial dilutions of NVP-BE2235 in the BC cell lines MDA-MB-231 (squares) and MCF-7 (triangles) under normoxic (filled symbols) and hypoxic conditions (empty symbols). The effect on cell viability was measured by standard MTS assay. The diagram represents the means of at least two independent experiments, each performed in triplicates, normalized against DMSO-treated controls. Dose–response curves were generated using the standard four parameter logistic models. Error bars indicate SD values.

hypoxic and reoxygenated samples (Fig. 4B). As expected, HIF-1 α expression was reduced in reoxygenated cells over time. Interestingly, prolonged incubation with NVP-BE2235 also somewhat decreased the HIF-1 α expression in hypoxic samples, as shown in Figure 4B and ESM Figure 1B.

Figure 4A shows representative normalized cell survival responses of drug-treated MCF-7 cells and DMSO-treated controls after IR with doses from 0 to 8 Gy under different oxygen conditions. The MDA-MB-231 cell line showed qualitative similar results (ESM Figure 1A). At least three independent experiments were performed, and the radiation dose yielding 10% survival (D10) and the surviving fraction at

2 Gy (SF2), as well as the plating efficiencies and the oxygen enhancement ratios for the D10 (OER D10) and the SF2 (OER SF2) are summarized in ESM Figure 2.

As apparent in ESM Figure 2, the plating efficiency was not significantly influenced by hypoxia or NVP-BE2235 in both cell lines. However, in both cell lines reoxygenated and hypoxic untreated cells were statistically significant more resistant to IR than normoxic cells. In both cell lines, the calculated OER D10 and OER SF2 were about 1.3 and 1.4 for hypoxic and reoxygenated cells, respectively (ESM Figure 2C–F). No significant changes between reoxygenated and hypoxic DMSO-treated cells were detected in both cell lines. Most strikingly,

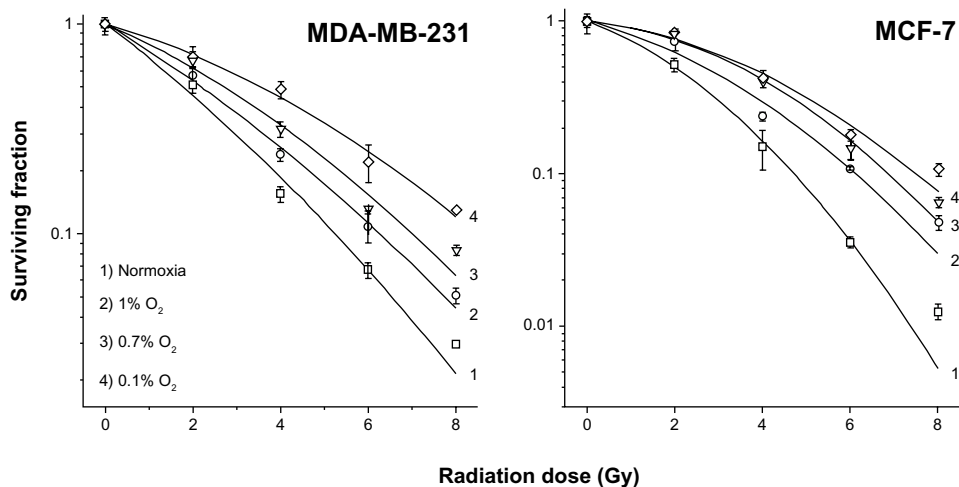


Figure 3. Representative colony-forming abilities of MDA-MB-231 and MCF-7 cancer cells cultivated and irradiated in 21% (1), 1% (2), 0.7% (3), or 0.1% (4) oxygen. Twenty-four hours after IR, cells were replated, and colonies were fixed and stained using standard protocols after two weeks.

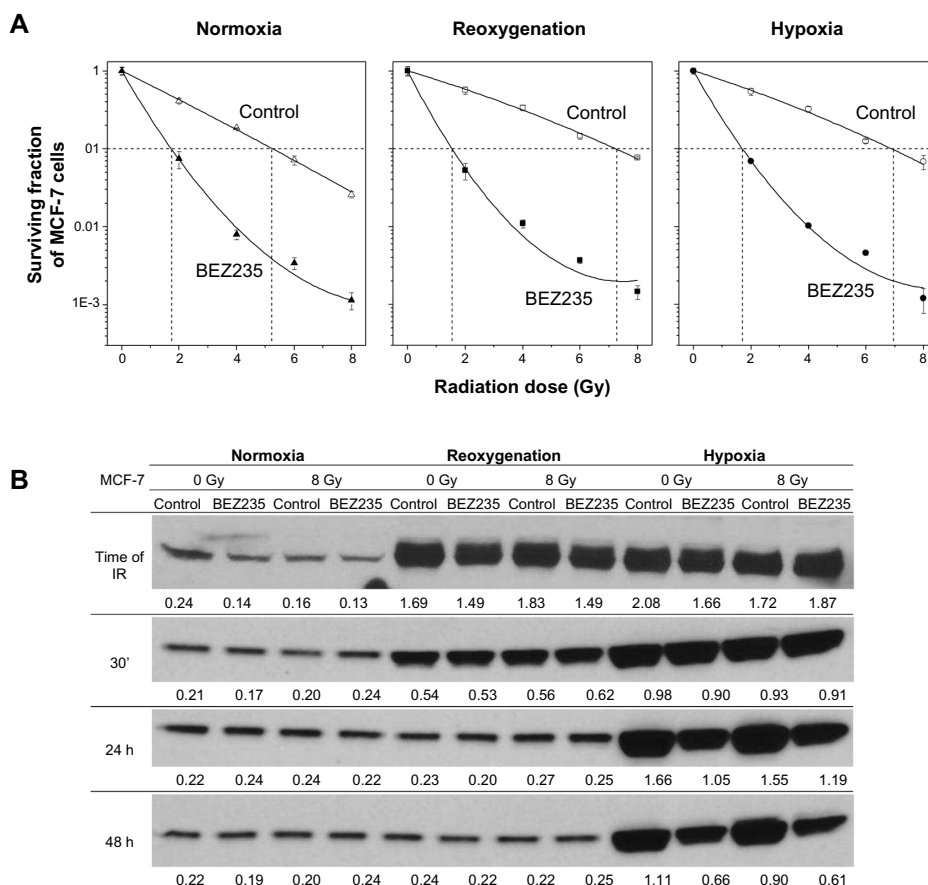


Figure 4. Representative colony-forming abilities of MCF-7 cancer cells treated with 100 nM NVP-BE2235 (filled symbols) or equal amounts of DMSO (empty symbols) before IR (A). Two weeks after IR, colonies were fixed and stained using standard protocols. Experiments were performed in quadruplicates, and colonies containing at least 50 cells were scored as survivors. The doses yielding 10% survival (D_{10}) are indicated by dotted lines. Representative expression of HIF-1 α protein in MCF-7 at the time of IR, 30 minutes, 24 hours, and 48 hours after IR (B). Cells were cultivated under normoxic, reoxygenated, or hypoxic conditions and treated with NVP-BE2235 or DMSO before IR with 8 Gy. Protein bands were normalized to the β -tubulin intensity, and changes in protein expression are denoted by numbers.

treatment with NVP-BE2235 statistically significant radiosensitized both cell lines independent of oxygen supply (Fig. 4A, ESM Figure 1A, and ESM Figure 2C–F). Moreover, treatment with the dual PI3K/mTOR inhibitor totally circumvented the negative effects of hypoxia on the radiosensitivity, as shown by almost equal D_{10} and SF2 values for NVP-BE2235-treated samples independent of their oxygenation status (ESM Figure 2C–F).

NVP-BE2235 suppresses activity of the PI3K/Akt/mTOR pathway. To investigate the molecular reasons for the NVP-BE2235-induced increased radiosensitivity of tumor cells, which was independent of cellular oxygenation status, we assessed the expression of several relevant proteins of the PI3K/Akt/mTOR signaling cascade after combined drug-IR treatment in normoxic, reoxygenated, and hypoxic cells.

As shown in Figure 5, incubation with NVP-BE2235 inactivated the PI3K/AKT/mTOR signaling cascade independent of cellular oxygenation status, as indicated by decreased phosphorylation of Akt, mTOR, S6, and 4E-BP1. This effect was observed up to 48 hours after IR in the MCF-7

cell line (ESM Figure 3A and B). None or only minor changes were observed in protein expression of PI3K subunits p110 and p85, AKT, mTOR, and S6.

In general, the MDA-MB-231 cells showed qualitatively similar data for the expression of the tested PI3K/Akt/mTOR pathway proteins, with the exception of p-Akt, which was not detectable in MDA-MB-231 cells. Furthermore, phosphorylation of mTOR was diminished 30 minutes after IR in NVP-BE2235-treated cells, but mTOR phosphorylation was not suppressed after prolonged incubation with NVP-BE2235 (ESM Figure 3C–E). However, as proven by diminished S6 and 4E-BP1 phosphorylation, treatment with NVP-BE2235 led to inactivation of mTOR signaling in both BC cell lines in all three oxygenation states tested in this study.

NVP-BE2235 induces programmed cell death and autophagy. To further elucidate the molecular reasons for the NVP-BE2235-mediated radiosensitization, we assessed the induction of programmed cell death in cells treated with the dual PI3K/mTOR inhibitor and IR under different oxygen conditions. Figure 6A summarizes three independent experiments and shows the mean percentage of cells with

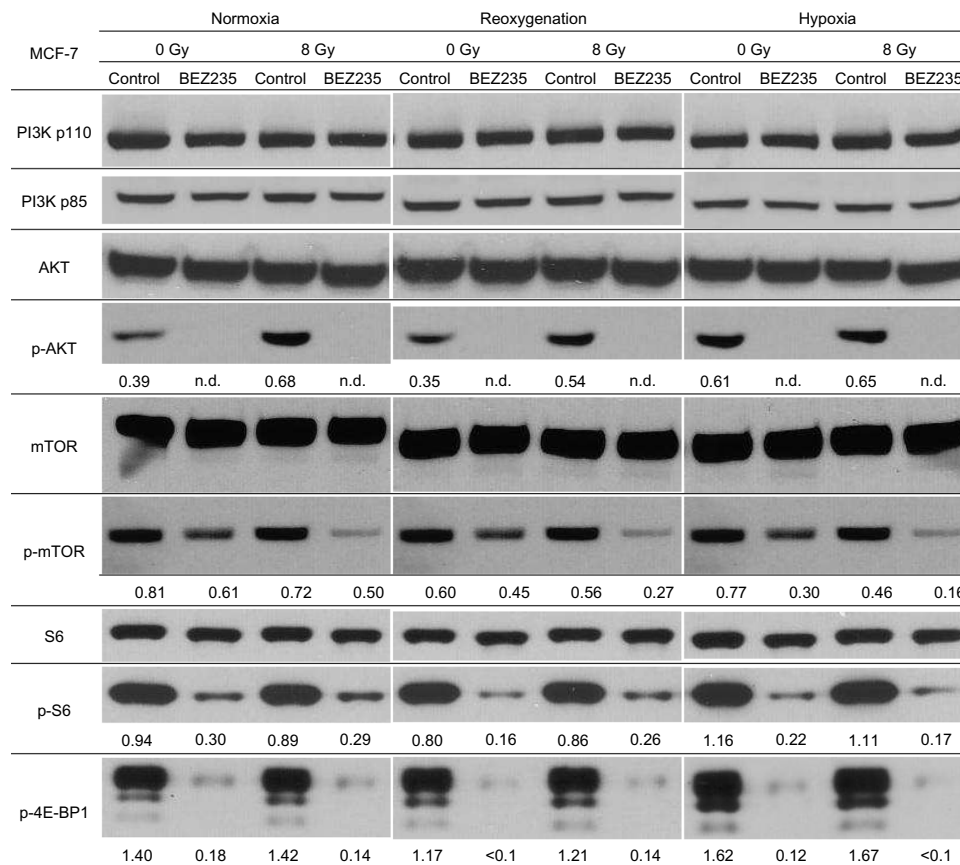


Figure 5. Representative Western blot analysis of expression levels of several marker proteins of the PI3K pathway in MCF-7 cellular lysates, prepared 30 minutes after IR. Cells were treated with NVP-BEZ235 or DMSO before IR at 8 Gy and cultivated under normoxic, reoxygenated, or hypoxic conditions. Protein bands were normalized to the β -actin intensity, and changes in protein expression are denoted by numbers. The experiment was repeated at least three times. n.d. indicates not determinable.

hypodiploid DNA content and cellular debris, a marker for late stage apoptosis, in MCF-7 cells 48 hours after IR. Cells were cultivated under normoxic, reoxygenated, and hypoxic conditions, and treated with NVP-BEZ235 (gray columns) one hour before IR with 8 Gy (striped columns). Oxygenation status did not affect late stage apoptosis in untreated and non-irradiated MCF-7 cells (white non-striped columns). However, exposing MCF-7 cells to IR caused a statistical significant increase in hypodiploid cells, indicating cell death, independent of oxygenation status.

Furthermore, treatment with the dual PI3K/mTOR inhibitor induced apoptosis as well, as shown by statistical significant increases in hypodiploid fractions at all oxygen conditions tested. Combining IR and NVP-BEZ235 treatment (gray striped column) enhanced cell death in the MCF-7 cell line independent of oxygenation status, as seen by a statistical significant increase in hypodiploid cells and cellular debris compared to IR or drug-treated cells alone.

As shown in ESM Figure 4A, the response of MDA-MB-231 cells was somewhat different. Treatment with NVP-BEZ235 did not cause any significant changes in the percentage of hypodiploid cells and debris in all oxygen conditions. However, exposing MDA-MB-231 cells to IR

increased apoptosis, but in contrast to MCF-7 cells, this apoptosis was not statistically significantly enhanced by dual PI3K/mTOR inhibition, although tendencies were noticeable.

Furthermore, we probed for the expression and cleavage of the DNA repair enzyme PARP and for expression of the autophagy markers LC3-I and LC3-II. Figure 6B and ESM Figure 4B show samples of MCF-7 and MDA-MB-231 cells, respectively, which were collected 48 hours after IR and cultivated in normoxic, reoxygenated, or hypoxic conditions. Treatment of the MCF-7 cell line with NVP-BEZ234 caused a decrease in PARP levels in all oxygen conditions, most likely by PARP degradation, indicated by increased cleaved PARP levels. In line with the previous shown data for late stage apoptosis (Fig. 6A), combined dual PI3K/mTOR inhibition and IR caused the highest levels of cleaved PARP.

To assess the impact of NVP-BEZ235 and IR on the induction of autophagy, we probed for the autophagy marker protein LC3, which is converted from the cytosolic soluble LC3-I to the membrane-bound LC3-II form during autophagy. As shown in Figure 6B, treatment of MCF-7 cells with NVP-BEZ235 caused a strong decrease in LC3-I

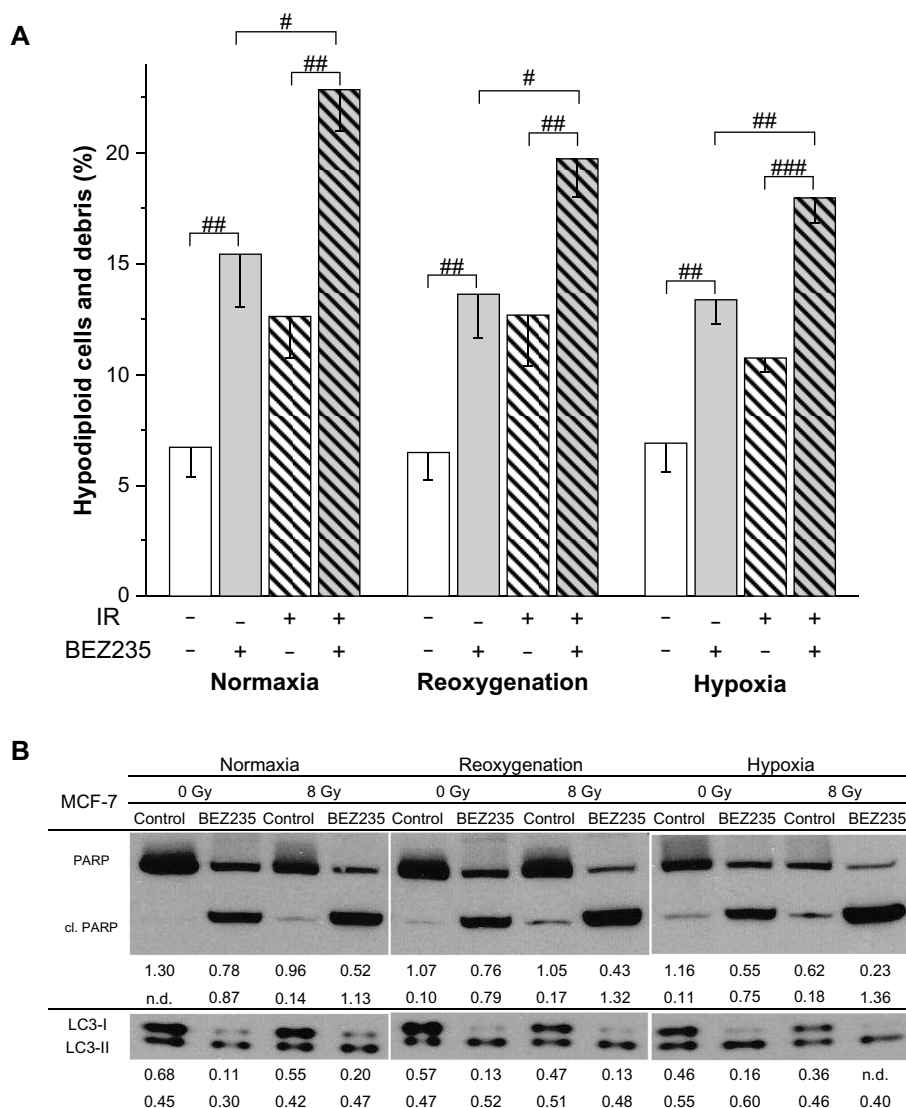


Figure 6. Mean percentage of cells with hypodiploid DNA content and cellular debris in NVP-BE235-treated (grey columns) and irradiated (striped columns) normoxic, reoxygenated, and hypoxic MCF-7 cells 48 hours after IR (A). DMSO-treated (white columns) and non-irradiated (non-striped columns) cells served as controls. Cells were detached with trypsin, fixed, permeabilized, stained with DAPI, and then analyzed for fluorescence by flow cytometry. The columns display means (\pm standard deviation) of hypodiploid nuclei and cellular debris of at least three independent experiments. Statistical comparisons between controls were omitted for reasons of clarity. Statistically significant differences are indicated as follows: # $P < 0.05$, ## $P < 0.01$, and ### $P < 0.001$. Representative Western blot analysis of expression levels of apoptosis and autophagy-relevant proteins in MCF-7 cellular lysates, prepared 48 hours after IR (B). Cells were cultivated under normoxic, reoxygenated, or hypoxic conditions and treated with NVP-BE235 or DMSO before IR at 8 Gy. Protein bands were normalized to the β -actin intensity, and changes in protein expression are denoted by numbers. The experiment was repeated at least three times. n.d. indicates not determinable.

48 hours after IR in all drug-treated samples, but no enrichment of LC3-II was observed.

ESM Figure 4B shows that the cellular response of MDA-MB-231 cells in terms of PARP expression and cleavage is also in line with the previous shown data for late stage apoptosis (ESM Figure 4A). Exposing MDA-MB-231 cells to IR caused a slight increase in PARP cleavage, but in contrast to the MCF-7 cell line, treatment with NVP-BE235 caused only minor changes in PARP cleavage independent of oxygenation status. However, NVP-BE235-mediated depletion of LC3-I

protein was observable 48 hours after IR in MDA-MB-231 cells in all tested oxygenation conditions as well (ESM Figure 4B).

Effect of oxygenation status, NVP-BE235, and IR on cell cycle and DNA damage. To further explore the molecular basis for the radiosensitizing effect of the dual PI3K/mTOR inhibitor, we assessed if cell cycle alterations and DNA DSBs were observable after NVP-BE235 treatment and/or IR. The summarized data for the cell cycle phase distributions and the normalized DNA DSBs of at least three independent experiments are shown in ESM Figure 5 and ESM Figure 6, respectively.

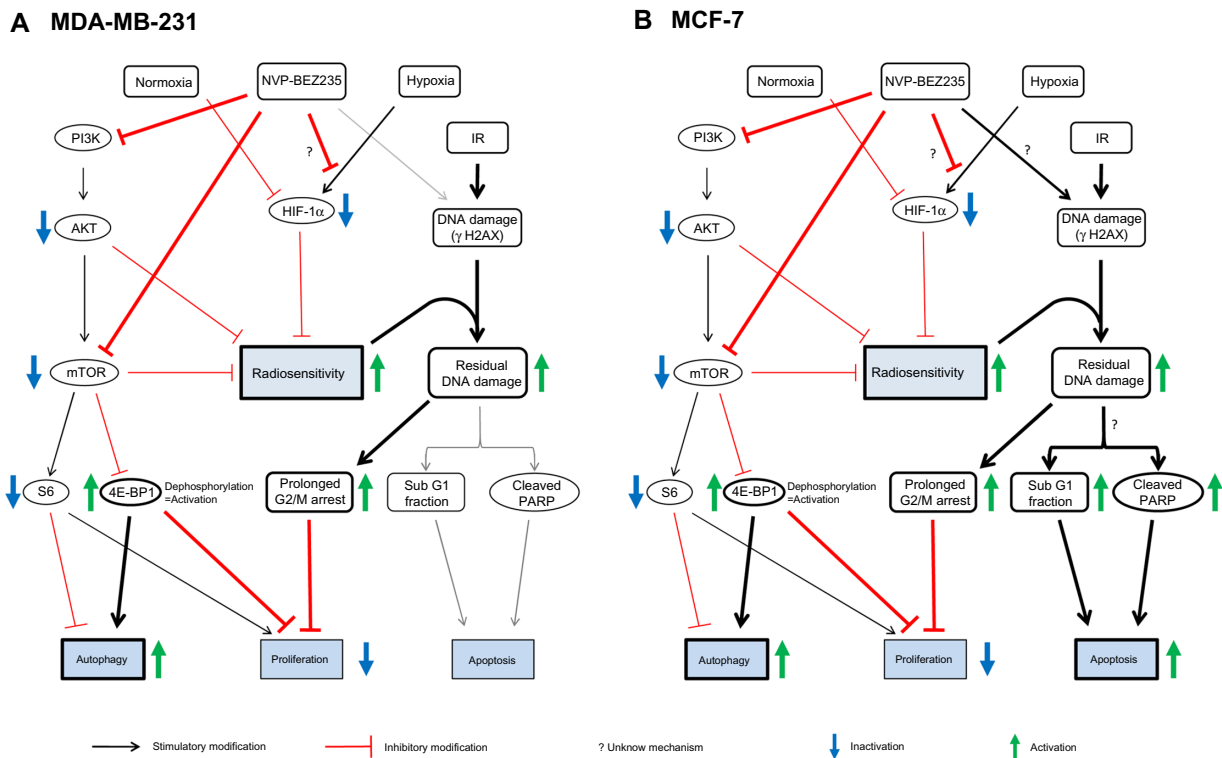


Figure 7. A simplified diagram of putative signaling pathways accounting for the radiosensitization of MDA-MB-231 (A) and MCF-7 cells (B) treated with the dual PI3K/mTOR inhibitor NVP-BE235 in normoxic and hypoxic conditions. Incubation of tumor cells with NVP-BE235 for one hour before and up to 48 hours after IR decreases HIF-1 α expression in hypoxic cells (Fig. 4 and ESM Figures 1 and 2), circumventing the negative effect of hypoxia in terms of radiosensitivity (Fig. 3). Furthermore, NVP-BE235 treatment inactivates the PI3K/AKT/mTOR signaling cascade, proven by dephosphorylation of AKT, mTOR, S6, and 4E-BP1 (Fig. 5 and ESM Figure 3), which in the case of 4E-BP1 causes an activation of the translational repressor protein. Inactivation of mTOR subsequently induces autophagy (Fig. 6B and ESM Figure 4B) and diminishes proliferation. Apart from these effects, dephosphorylation of AKT and mTOR by NVP-BE235 increases radiosensitivity. This increase in radiosensitivity, caused by reduction in HIF-1 α expression, inactivation of the PI3K/AKT/mTOR signaling cascade, and may be also by other not yet identified NVP-BE235-induced mechanisms, causes an increase in residual DNA damages (detected by γ H2AX immunofluorescence) after IR (ESM Figure 6). These unrepaired, IR-induced DNA damages subsequently result in a prolonged G2/M-phase arrest (ESM Figure 5), which further diminishes proliferation. Apart from the effects already mentioned for the MDA-MB-231 cell line, prolonged incubation with NVP-BE235 induces DNA damages (ESM Figure 6) and enhances IR-induced apoptosis in MCF-7 cells (Fig. 6).

As expected, neither NVP-BE235 nor IR had effects on the cell cycle phase distribution 30 minutes after IR (ESM Figure 5). After 24 hours, the response to IR was different in the two cell lines. While MDA-MB-231 cells accumulated in the G2/M-phase, MCF-7 cells were arrested in the G1-phase. However, 48 hours after IR, the cell cycle phase distribution of irradiated control cells began to normalize, whereas in NVP-BE235-treated cells a significant higher amount of G2/M-phase cells was detected. This indicated a stable G2/M-phase arrest. Furthermore, we observed an arrest of non-irradiated cells in the G1-phase after prolonged incubation with the dual PI3K/mTOR inhibitor in both cell lines independent of oxygenation status.

As shown in ESM Figure 6, treatment of cells with NVP-BE235 caused diminished H2AX phosphorylation 30 minutes after IR, representing less DNA damage than in irradiated control cells. However, with increasing repair time, DNA DSBs' content was significantly higher in NVP-BE235-treated and irradiated cells compared to irradiated

controls, indicating protracted DNA repair. Noteworthy, and in line with the results of the apoptosis assays, prolonged incubation of MCF-7 cells with NVP-BE235 caused a γ H2AX increase in non-irradiated cells. All the aforementioned effects on DNA damage induction and repair were observed independent of the oxygenation condition.

Discussion

Targeting the anti-apoptotic PI3K/AKT/mTOR pathway to improve cancer control has been an intense and promising research field within the last decades. However, first-generation inhibitors of this pathway, such as wortmannin, LY294002, or rapamycin and its derivatives, demonstrated undesirable side effects and low specificity in some experiments.³²⁻³⁴ Therefore, second-generation inhibitors with improved specificity and pharmacological properties have been developed and are in clinical trials currently.^{26,35,36} One of these second-generation inhibitors is the novel orally available dual PI3K/mTOR inhibitor NVP-BE235. This imidazo[4,5-c]quinoline derivative



demonstrated anti-proliferative and radiosensitizing activity in various *in vitro* and *in vivo* studies.^{24,27,31,37–44} Although, there is evidence that NVP-BEZ235 is able to sensitize fibrosarcoma as well as pharynx and prostate carcinoma cells to IR in normoxic and harsh hypoxic conditions,^{24,25} up-to-date no data are available about the radiosensitizing potential of NVP-BEZ235 in BC cell lines.

This study was designed to prove whether treatment with the dual PI3K/mTOR inhibitor NVP-BEZ235 sensitizes the TN BC cell line MDA-MB-231 and the ER-positive cell line MCF-7 to IR in three different clinically relevant oxygen conditions: normoxic, reoxygenated after IR, and hypoxic.

The observed effects of NVP-BEZ235-mediated radiosensitization are summarized as a schematic pathway in Figure 7.

In our experiments, treatment with the dual inhibitor reduced carbonic anhydrase 9 (data not shown) and HIF-1 α (Fig. 4) expression in hypoxic cells, which is in line with previous results.⁴⁵ This is of utmost interest, because HIF-1 α is a promising target for radiosensitization of tumors.^{13,46} Fokas et al. recently showed that dual PI3K/mTOR inhibition normalized the aberrant vascular system in tumor xenografts.²⁴ However, apart from normalizing the vascular system, the exact molecular mechanism, in which the PI3K/AKT/mTOR pathway regulates HIF-1 α expression, is not completely understood yet. As our *in vitro* data show that inhibition of HIF-1 α is also an important feature of NVP-BEZ235-mediated radiosensitization of hypoxic cells, this effect is worth to be evaluated in future experiments.

Another prime target for radiosensitizing approaches is the PI3K/AKT/mTOR pathway, which is activated in the majority of cancers.^{5,47} As shown, treatment with the dual inhibitor caused dephosphorylation of AKT, mTOR, S6, and 4E-BP1, which in the case of 4E-BP1 causes activation of the translational repressor protein. Especially, AKT and mTOR have been shown to promote cellular survival and radioresistance in various setups.^{48,49} Noteworthy, the inactivation of AKT was stable in the MCF-7 cell line. This is of certain interest, because various studies report an upregulation of p-AKT after prolonged incubation with the dual inhibitor,^{27,31,39,50,51} undermining the potential of NVP-BEZ235 in these setups. In addition to the stable AKT inhibition, activating PI3K mutations are the most common (up to 40%) genetic aberrations in primary BC.⁵² This provides a further rationale for targeting the PI3K/AKT/mTOR axis in BC. Therefore, concomitant treatment with NVP-BEZ235 and IR has the potential to greatly improve therapy outcome in a large set of BC patients.

Whereas we observed apoptosis in the MCF-7 cell line after prolonged NVP-BEZ235 treatment at all tested oxygen conditions, no such apoptosis induction was observable in the MDA-MB-231 cell line. This is most likely because of the combination of the aforementioned inhibition of AKT, which was only observed in MCF-7 cells and which has been

shown to induce cell death in several experiments^{53–55} and a non-mutated version of the *p53* gene in the MCF-7 cell line. The fact that, unlike to most other solid human malignancies, mutations of the *p53* gene occur with an inferior frequency in BC⁵⁶ further supports the potential of NVP-BEZ235 in BC treatment.

Apart from the induction of cell death, which was dependent of the mutational status, we observed induction of autophagy in both cell lines after NVP-BEZ235 treatment in all tested oxygen conditions. In contrast to the current paradigm of autophagy, in which accumulation of LC3-II protein occurs,^{57,58} we observed a strong reduction in LC3-I but no increase in LC3-II levels. However, Mizushima and Yoshimori recently reported that the initially increased LC3-II level is degraded within a few hours after autophagy induction by delivery of LC-II to lysosomes.⁵⁹ The induction of autophagy by NVP-BEZ235 is of interest, because its role in cancer is not completely understood yet, and this cellular process is highly discussed in the current literature.^{60,61} Several research groups aimed to exploit the autophagic process by inhibiting lysosomal degradation with bafilomycin A1 or chloroquine, which was shown to sensitize cells to IR.^{62–64} Whether simultaneous blockade of autophagy can enhance the NVP-BEZ235-mediated radiosensitization of BC cell lines will be explored in future experiments to further enhance the radiosensitizing potential of NVP-BEZ235.

In addition to the aforementioned results, we observed reduced initial phosphorylation of H2AX along with reduced DNA repair after combined NVP-BEZ235 IR treatment. One possible explanation for these diminished initial DNA damages and their resolution in NVP-BEZ235-treated cells is the inhibition of DNA-PK, ATR, and ATM kinases as side targets of the dual inhibitor.^{43,65,66} Activation of these kinases is part of the DNA damage response and is involved in both formation and resolution of γ H2AX.^{67,68} Therefore, their inhibition can explain both the impaired induction and the protracted repair of DNA DSB. The fact that 24 hours after IR no differences between irradiated drug and DMSO-treated hypoxic cells were observed most likely is caused by reduced DNA repair mechanisms in hypoxic cells as reported elsewhere.^{69,70} However, as reported by various research groups, inhibition of DNA repair mechanisms sensitized tumor cells to cytotoxic agents as IR.^{71–73} We therefore conclude, that DNA repair protraction, which was observed in all tested oxygen conditions, might be another hallmark of radiosensitization of the BC cell lines.

To sum up, treatment with the dual PI3K/mTOR inhibitor radiosensitized the TN MDA-MB-231 and the ER-positive MCF-7 cell line in different physiological relevant oxygenation states, namely normoxic, reoxygenated after IR, and hypoxic. This oxygen-independent radiosensitization is most likely caused by inhibition of HIF-1 α and PI3K/AKT/mTOR signaling, DNA repair impairment, autophagy, and some extent induction of apoptosis. Furthermore, combined



drug-IR treatment decreased proliferation in both cell lines to a greater extent, than each treatment alone, indicating additive or synergistic effects. NVP-BEZ235 is in clinical trial phase I/II studies at the moment and especially the promising results in MCF-7 cells, along with the fact that the majority of human BCs are ER positive⁷⁴ and harbor PI3K activating mutations but are p53 wild-type,^{52,56} indicate a clinically relevant application of NVP-BEZ235 in BC radiotherapy.

Acknowledgment

We thank Gerald Büchold for the construction of the IR device.

Author Contributions

CSD and SK conceived and designed the experiments. SK, EC, BP, UK, MF, and CSD analyzed the data. SK and CSD wrote the first draft of the manuscript. SK, CSD, UK, and MF contributed to the writing of the manuscript. SK, EC, BP, UK, MF, and CSD agreed with manuscript results and conclusions. SK, CSD, UK, and MF jointly developed the structure and arguments for the paper. SK, CSD, UK, BP, and MF made critical revisions and approved the final version. All authors reviewed and approved the final manuscript.

DISCLOSURES AND ETHICS

As a requirement of publication the authors have provided signed confirmation of their compliance with ethical and legal obligations including but not limited to compliance with ICMJE authorship and competing interests guidelines, that the article is neither under consideration for publication nor published elsewhere, of their compliance with legal and ethical guidelines concerning human and animal research participants (if applicable), and that permission has been obtained for reproduction of any copyrighted material. This article was subject to blind, independent, expert peer review. The reviewers reported no competing interests.

Supplementary Data

Supplementary file 1. This file contains further information about antibodies used.

Supplementary file 2. This file contains Supplementary Figures 1–6, as follows:

ESM figure 1. Representative colony forming abilities of MDA-MB-231 cancer cells treated with 100 nM NVP-BEZ235 (filled symbols) or equal amounts of DMSO (empty symbols) prior to IR (A).

ESM figure 2. Means (\pm standard deviation) of plating efficiencies (A and B), surviving fraction at 2 Gy (C and D) and dose yielding 10% survival (E and F) of MDA-MB-231 (A, C and E) and MCF-7 (B, D and F).

ESM figure 3. Representative Western blot analysis of expression levels of several marker proteins of the PI3K pathway in MCF-7 (A and B) and MDA-MB-231 (C-E) cellular lysates, prepared thirty minutes (C), 24 h (A and D) and 48 h (B and E) after IR.

ESM figure 4. Mean percentage of cells with hypodiploid DNA content and cellular debris in NVP-BEZ235 treated (grey columns) and irradiated (striped columns) normoxic,

reoxygenated and hypoxic MDA-MB-231 cells 48 h after IR (A).

ESM figure 5. Cell cycle phase distribution in MDA-MB-231 (A) and MCF-7 (B) tumor cells treated with NVP-BEZ235 and IR under different oxygen conditions.

ESM figure 6. DNA DSBs as detected by phosphorylation of the histone H2AX in MDAMB-231 (A) And MCF-7 (B) tumor cells treated with NVP-BEZ235 (grey columns) and IR (striped columns) under different oxygen conditions.

REFERENCES

- Howard JH, Bland KI. Current management and treatment strategies for breast cancer. *Curr Opin Obstet Gynecol.* 2012;24(1):44–8.
- Breast Cancer Treatment (PDQ®)—National Cancer Institute. Available at: <http://www.cancer.gov/cancertopics/pdq/treatment/breast/Patient/page5>. Accessed July 25, 2013.
- Cleator S, Heller W, Coombes RC. Triple-negative breast cancer: therapeutic options. *Lancet Oncol.* 2007;8(3):235–44.
- Reis-Filho JS, Tutt ANJ. Triple negative tumors: a critical review. *Histopathology.* 2008;52(1):108–18.
- Bartholomeusz C, Gonzalez-Angulo AM. Targeting the PI3K signaling pathway in cancer therapy. *Expert Opin Ther Targets.* 2012;16(1):121–30.
- Dillon RL, White DE, Muller WJ. The phosphatidylinositol 3-kinase signaling network: implications for human breast cancer. *Oncogene.* 2007;26(9):1338–45.
- Castaneda CA, Cortes-Funes H, Gomez HL, Ciruelos EM. The phosphatidylinositol 3-kinase/AKT signaling pathway in breast cancer. *Cancer Metastasis Rev.* 2010;29(4):751–9.
- Vaupel P, Schlenger K, Knoop C, Höckel M. Oxygenation of human tumors: evaluation of tissue oxygen distribution in breast cancers by computerized O₂ tension measurements. *Cancer Res.* 1991;51(12):3316–22.
- Ward C, Langdon SP, Mullen P, et al. New strategies for targeting the hypoxic tumour microenvironment in breast cancer. *Cancer Treat Rev.* 2013;39(2):171–9.
- Chaudary N, Hill RP. Hypoxia and metastasis in breast cancer. *Breast Dis.* 2006;26:55–64.
- Wilson WR, Hay MP. Targeting hypoxia in cancer therapy. *Nat Rev Cancer.* 2011;11(6):393–410.
- Bristow RG, Hill RP. Hypoxia and metabolism. Hypoxia, DNA repair and genetic instability. *Nat Rev Cancer.* 2008;8(3):180–92.
- Meijer TWH, Kaanders JHAM, Span PN, Bussink J. Targeting hypoxia, HIF-1, and tumor glucose metabolism to improve radiotherapy efficacy. *Clin Cancer Res.* 2012;18(20):5585–94.
- Pigott KH, Hill SA, Chaplin DJ, Saunders MI. Microregional fluctuations in perfusion within human tumours detected using laser Doppler flowmetry. *Radiother Oncol.* 1996;40(1):45–50.
- Iizuka M, Ando K, Aruga T, et al. Effects of reoxygenation on repair of potentially lethal radiation damage in cultured MG-63 osteosarcoma cells. *Radiat Res.* 1997;147(2):179–84.
- Urano M, Li GC, He F, Minami A, Burgman P, Ling CC. The effect of DN (dominant-negative) Ku70 and reoxygenation on hypoxia cell-kill: evidence of hypoxia-induced potentially lethal damage. *Int J Radiat Biol.* 2012;88(7):515–22.
- Pajonk F, Vlasi E, McBride WH. Radiation resistance of cancer stem cells: the 4 R's of radiobiology revisited. *Stem Cells.* 2010;28(4):639–48.
- Cam H, Houghton PJ. Regulation of mammalian target of rapamycin complex 1 (mTORC1) by hypoxia: causes and consequences. *Target Oncol.* 2011;6(2):95–102.
- Knaup KX, Jozefowski K, Schmidt R, et al. Mutual regulation of hypoxia-inducible factor and mammalian target of rapamycin as a function of oxygen availability. *Mol Cancer Res.* 2009;7(1):88–98.
- Wang Y, Ohh M. Oxygen-mediated endocytosis in cancer. *J Cell Mol Med.* 2010;14(3):496–503.
- Search of: BEZ235—List Results—ClinicalTrials.gov. Available at: <http://clinicaltrials.gov/ct2/results?term=bez235&Search=Search>. Accessed July 25, 2013.
- Leung E, Kim JE, Rewcastle GW, Finlay GJ, Baguley BC. Comparison of the effects of the PI3K/mTOR inhibitors NVP-BEZ235 and GSK2126458 on tamoxifen-resistant breast cancer cells. *Cancer Biol Ther.* 2011;11(11):938–46.
- Montero JC, Eparis-Ogando A, Re-Louhau MF, et al. Active kinase profiling, genetic and pharmacological data define mTOR as an important common target in triple-negative breast cancer. *Oncogene.* 2012;33(2):148–56.
- Fokas E, Im JH, Hill S, et al. Dual inhibition of the PI3K/mTOR pathway increases tumor radiosensitivity by normalizing tumor vasculature. *Cancer Res.* 2012;72(1):239–48.



25. Potiron VA, Abderrhamani R, Giang E, et al. Radiosensitization of prostate cancer cells by the dual PI3K/mTOR inhibitor BEZ235 under normoxic and hypoxic conditions. *Radiother Oncol J Eur Soc Ther Radiol Oncol*. 2013;106(1):138–46.
26. Maira S-M, Stauffer F, Bruggen J, et al. Identification and characterization of NVP-BEZ235, a new orally available dual phosphatidylinositol 3-kinase/mammalian target of rapamycin inhibitor with potent in vivo antitumor activity. *Mol Cancer Ther*. 2008;7(7):1851–63.
27. Kuger S, Graus D, Brendtke R, et al. Radiosensitization of glioblastoma cell lines by the dual PI3K and mTOR inhibitor NVP-BEZ235 depends on drug-irradiation schedule. *Transl Oncol*. 2013;6(2):169–79.
28. Franken NAP, Rodermond HM, Stap J, Haveman J, van Bree C. Clonogenic assay of cells in vitro. *Nat Protoc*. 2006;1(5):2315–9.
29. Rogakou EP, Pilch DR, Orr AH, Ivanova VS, Bonner WM. DNA double-stranded breaks induce histone H2AX phosphorylation on serine 139. *J Biol Chem*. 1998;273(10):5858–68.
30. Muslimovic A, Ismail IH, Gao Y, Hammarsten O. An optimized method for measurement of gamma-H2AX in blood mononuclear and cultured cells. *Nat Protoc*. 2008;3(7):1187–93.
31. Manara MC, Nicoletti G, Zambelli D, et al. NVP-BEZ235 as a new therapeutic option for sarcomas. *Clin Cancer Res*. 2010;16(2):530–40.
32. Markman B, Dienstmann R, Taberero J. Targeting the PI3K/Akt/mTOR pathway—beyond rapalogs. *Oncotarget*. 2010;1(7):530–43.
33. Prevo R, Deutsch E, Sampson O, et al. Class I PI3 kinase inhibition by the pyridinylfuranopyrimidine inhibitor PI-103 enhances tumor radiosensitivity. *Cancer Res*. 2008;68(14):5915–23.
34. Wan X, Harkavy B, Shen N, Grohar P, Helman LJ. Rapamycin induces feedback activation of Akt signaling through an IGF-1R-dependent mechanism. *Oncogene*. 2006;26(13):1932–40.
35. Fan Q-W, Knight ZA, Goldenberg DD, et al. A dual PI3 kinase/mTOR inhibitor reveals emergent efficacy in glioma. *Cancer Cell*. 2006;9(5):341–9.
36. Kurtz J-E, Ray-Coquard I. PI3 kinase inhibitors in the clinic: an update. *Anticancer Res*. 2012;32(7):2463–70.
37. Cho DC, Cohen MB, Panka DJ, et al. The efficacy of the novel dual PI3-kinase/mTOR inhibitor NVP-BEZ235 compared with rapamycin in renal cell carcinoma. *Clin Cancer Res*. 2010;16(14):3628–38.
38. Kong D, Dan S, Yamazaki K, Yamori T. Inhibition profiles of phosphatidylinositol 3-kinase inhibitors against PI3K superfamily and human cancer cell line panel JFCR39. *Eur J Cancer*. 2010;46(6):1111–21.
39. Liu T-J, Koul D, LaFortune T, et al. NVP-BEZ235, a novel dual phosphatidylinositol 3-kinase/mammalian target of rapamycin inhibitor, elicits multifaceted antitumor activities in human gliomas. *Mol Cancer Ther*. 2009;8(8):2204–10.
40. Santiskulvong C, Konecny GE, Fekete M, et al. Dual targeting of phosphoinositide 3-kinase and mammalian target of rapamycin using NVP-BEZ235 as a novel therapeutic approach in human ovarian carcinoma. *Clin Cancer Res*. 2011;17(8):2373–84.
41. Fokas E, Yoshimura M, Prevo R, et al. NVP-BEZ235 and NVP-BGT226, dual phosphatidylinositol 3-kinase/Mammalian target of rapamycin inhibitors, enhance tumor and endothelial cell radiosensitivity. *Radiat Oncol*. 2012;7(1):48.
42. Konstantinidou G, Bey EA, Rabellino A, et al. Dual phosphoinositide 3-kinase/mammalian target of rapamycin blockade is an effective radiosensitizing strategy for the treatment of non-small cell lung cancer harboring K-RAS mutations. *Cancer Res*. 2009;69(19):7644–52.
43. Mukherjee B, Tomimatsu N, Amancerla K, Camacho CV, Pichamoorthy N, Burma S. The dual PI3K/mTOR inhibitor NVP-BEZ235 is a potent inhibitor of ATM- and DNA-PKcs-mediated DNA damage responses. *Neoplasia*. 2012;14(1):34–43.
44. Zhu W, Fu W, Hu L. NVP-BEZ235, dual phosphatidylinositol 3-kinase/mammalian target of rapamycin inhibitor, prominently enhances radiosensitivity of prostate cancer cell line PC-3. *Cancer Biother Radiopharm*. 2013;28(9):665–73.
45. Karar J, Cerniglia GJ, Lindsten T, Koumenis C, Maity A. Dual PI3K/mTOR inhibitor NVP-BEZ235 suppresses hypoxia-inducible factor (HIF)-1 α expression by blocking protein translation and increases cell death under hypoxia. *Cancer Biol Ther*. 2012;13(11):1102–11.
46. Moeller BJ, Dewhirst MW. HIF-1 and tumour radiosensitivity. *Br J Cancer*. 2006;95(1):1–5.
47. Courtney KD, Corcoran RB, Engelman JA. The PI3K pathway as drug target in human cancer. *J Clin Oncol*. 2010;28(6):1075–83.
48. Chautard E, Loubeau G, Tchirkov A, et al. Akt signaling pathway: a target for radiosensitizing human malignant glioma. *Neuro Oncol*. 2010;12(5):434–43.
49. Gupta AK, Cerniglia GJ, Mick R, et al. Radiation sensitization of human cancer cells in vivo by inhibiting the activity of PI3K using LY294002. *Int J Radiat Oncol Biol Phys*. 2003;56(3):846–53.
50. Masuda M, Shimomura M, Kobayashi K, Kojima S, Nakatsura T. Growth inhibition by NVP-BEZ235, a dual PI3K/mTOR inhibitor, in hepatocellular carcinoma cell lines. *Oncol Rep*. 2011;26(5):1273–9.
51. Roper J, Richardson MP, Wang WV, et al. The dual PI3K/mTOR inhibitor NVP-BEZ235 induces tumor regression in a genetically engineered mouse model of PIK3CA wild-type colorectal cancer. *PLoS ONE*. 2011;6(9):e25132.
52. Campbell IG, Russell SE, Choong DYH, et al. Mutation of the PIK3CA gene in ovarian and breast cancer. *Cancer Res*. 2004;64(21):7678–81.
53. Bjornsti M-A, Houghton PJ. The TOR pathway: a target for cancer therapy. *Nat Rev Cancer*. 2004;4(5):335–48.
54. Nakashio A, Fujita N, Rokudai S, Sato S, Tsuruo T. Prevention of phosphatidylinositol 3'-kinase-Akt survival signaling pathway during topotecan-induced apoptosis. *Cancer Res*. 2000;60(18):5303–9.
55. Vivanco I, Sawyers CL. The phosphatidylinositol 3-kinase AKT pathway in human cancer. *Nat Rev Cancer*. 2002;2(7):489–501.
56. Gasco M, Shami S, Crook T. The p53 pathway in breast cancer. *Breast Cancer Res*. 2002;4(2):70–6.
57. Barth S, Glick D, Macleod KF. Autophagy: assays and artifacts. *J Pathol*. 2010;221(2):117–24.
58. Tanida I, Ueno T, Kominami E. LC3 and autophagy. *Methods Mol Biol*. 2008;445:77–88.
59. Mizushima N, Yoshimori T. How to interpret LC3 immunoblotting. *Autophagy*. 2007;3(6):542–5.
60. Hippert MM, O'Toole PS, Thorburn A. Autophagy in cancer: good, bad, or both? *Cancer Res*. 2006;66(19):9349–51.
61. Roy S, Debnath J. Autophagy and tumorigenesis. *Semin Immunopathol*. 2010;32(4):383–96.
62. Apel A, Herr I, Schwarz H, Rodemann HP, Mayer A. Blocked autophagy sensitizes resistant carcinoma cells to radiation therapy. *Cancer Res*. 2008;68(5):1485–94.
63. Krakstad C, Chekenya M. Survival signalling and apoptosis resistance in glioblastomas: opportunities for targeted therapeutics. *Mol Cancer*. 2010;9(1):135.
64. Zhuang W, Qin Z, Liang Z. The role of autophagy in sensitizing malignant glioma cells to radiation therapy. *Acta Biochim Biophys Sin (Shanghai)*. 2009;41(5):341–51.
65. Shortt J, Martin BP, Newbold A, et al. Combined inhibition of PI3K-related DNA damage response kinases and mTORC1 induces apoptosis in MYC-driven B-cell lymphomas. *Blood*. 2013;121(15):2964–74.
66. Toledo LI, Murga M, Zur R, et al. A cell-based screen identifies ATR inhibitors with synthetic lethal properties for cancer-associated mutations. *Nat Struct Mol Biol*. 2011;18(6):721–7.
67. Kinner A, Wu W, Staudt C, Iliakis G. Gamma-H2AX in recognition and signaling of DNA double-strand breaks in the context of chromatin. *Nucleic Acids Res*. 2008;36(17):5678–94.
68. Shiloh Y, Ziv Y. The ATM protein kinase: regulating the cellular response to genotoxic stress, and more. *Nat Rev Mol Cell Biol*. 2013;14(4):197–210.
69. Bindra RS, Crosby ME, Glazer PM. Regulation of DNA repair in hypoxic cancer cells. *Cancer Metastasis Rev*. 2007;26(2):249–60.
70. Kumareswaran R, Ludkovski O, Meng A, Sykes J, Pintilie M, Bristow RG. Chronic hypoxia compromises repair of DNA double-strand breaks to drive genetic instability. *J Cell Sci*. 2012;125(Pt 1):189–99.
71. Dumont F, Altmeyer A, Bischoff P. Radiosensitising agents for the radiotherapy of cancer: novel molecularly targeted approaches. *Expert Opin Ther Pat*. 2009;19(6):775–99.
72. Fuhrman CB, Kilgore J, LaCoursiere YD, et al. Radiosensitization of cervical cancer cells via double-strand DNA break repair inhibition. *Gynecol Oncol*. 2008;110(1):93–8.
73. Senra JM, Telfer BA, Cherry KE, et al. Inhibition of PARP-1 by olaparib (AZD2281) increases the radiosensitivity of a lung tumor xenograft. *Mol Cancer Ther*. 2011;10(10):1949–58.
74. Castoria G, Migliaccio A, Giovannelli P, Auricchio F. Cell proliferation regulated by estradiol receptor: therapeutic implications. *Steroids*. 2010;75(8–9):524–7.